Catalysis Today 158 (2010) 305–309

Contents lists available at ScienceDirect

Catalysis Today

journal homepage: www.elsevier.com/locate/cattod

Catalytic activity of core–shell structured Cu/Fe_3O_4@SiO_2 microsphere catalysts

Junhong Ji[a], Penghui Zeng[a,b], Shengfu Ji[a,*], Wei Yang[a], Hongfei Liu[a], Yingyi Li[a]

[a] State Key Laboratory of Chemical Resource Engineering, Beijing University of Chemical Technology, Beijing 100029, China
[b] State Key Laboratory of Heavy Oil Processing, China University of Petroleum, Beijing 102200, China

ARTICLE INFO

Keywords:
Core–shell structured
Nano-Cu
Microsphere catalysts
Formaldehyde
Hydrogen

ABSTRACT

The core–shell structured Cu/Fe_3O_4@SiO_2 catalysts were prepared via two steps. First, the Fe_3O_4@SiO_2 microspheres were synthesized using the nano-Fe_3O_4 as the core, TEOS as silica source, and CTAB as surfactant. Second, the Cu nano-grains, obtained by reducing copper ammonia complexes with hydrazine hydrate, were supported on the surface of the Fe_3O_4@SiO_2 microspheres. The structure of the samples was characterized by X-ray diffraction (XRD), transmission electron microscopy (TEM), N_2 adsorption–desorption isotherms and vibration sample magnetometer (VSM). The catalytic activity of Cu/Fe_3O_4@SiO_2 catalysts for the production of hydrogen from low concentration formaldehyde solution was evaluated. The results indicated that the size of the Fe_3O_4@SiO_2 and the Cu/Fe_3O_4@SiO_2 was about 500 nm. The diameter of Cu particles on the surface of Cu/Fe_3O_4@SiO_2 was 10 nm. Both the Fe_3O_4@SiO_2 and the Cu/Fe_3O_4@SiO_2 had the mesoporous structure. The samples presented the superparamagnetism at room temperature. The low concentration formaldehyde could be effectively converted into hydrogen at room temperature. The Cu/Fe_3O_4@SiO_2 with Cu content 15 wt% exhibited the best catalytic performance. The accumulative amount of H_2 reached 42 mL in 45 min. After reaction recycling for 8 times, the catalytic activity of the catalyst had not been obviously dropped.

1. Introduction

The development of more efficient and stable catalysts has been an increasingly important goal for chemists and material scientists for both economic and environmental reasons. Recently, more attention has been paid to the magnetic core–shell structure nano-composites due to their unique magnetic properties. Usually, industrial catalytic reactions were performed in liquid phase. The recycle use of the solid catalyst was very difficult. If core–shell structure composites use magnetic catalysts with the Fe_3O_4 core and the SiO_2 shell, the recycle use of the catalysts can be carried out under the magnetic field. Hence, the magnetic core–shell structure composites were not only an effective material for water treatment, but also a good support for the catalysts [1–3].

More recently, Marcos et al. used the Fe_3O_4/SiO_2 as support, by reducing $Fe_3O_4/SiO_2–NH_2–Ru(III)$ with $NaBH_4$, obtained the Fe_3O_4/SiO_2 supported Ru catalysts. The catalytic hydrogenation reaction of 1-phenylethanol showed that the catalyst could be reused up to 3 times for successive oxidation reactions without changing the conversion of the reaction (>99% conversion) [4,5]. Ge et al. [6] had synthesized the core–shell structure catalysts with active component Au nano-grains protected within porous SiO_2 shells. The catalysts were used in the reduction reaction of 4-nitrophenol by $NaBH_4$. The conversion of 4-nitrophenol still maintained 70% when the catalysts were reused for 6 times.

In some chemical processes, for example, the organic synthesis, synthetic fiber, textile processing, wood processing, and painting, the formaldehyde has often been emitted. Because of the large water-solubility of the formaldehyde, the wastewater of these chemical processes generally contains the low concentration formaldehyde (0.2–4.0 g/L), and sometimes even more than 10 g/L. It brings greater harm to environment and human health [7]. Hence, seeking an effective way for the elimination formaldehyde of industrial wastewater is particularly necessary. At present, many literature had reported that formaldehyde can be effectively adsorbed on metallic nanoparticles or its oxide. Millar et al. [8] found that formaldehyde can be effectively adsorbed on the Cu/SiO_2 catalyst, and polymerized formaldehyde observed. Hung and Bernasek [9] found that formaldehyde can be adsorbed in the Fe (1 0 0) surface when the temperature was below 220 K. Stadler et al. [10] showed that the formaldehyde can be adsorbed on Au (1 1 1) surface. In addition, there are similar reports about absorption of formaldehyde on the surface of CeO_2, TiO_2, and Pt [11–14]. In particular, Bi and Lu [15] reported that the low concentration formaldehyde can be catalyzed by nano-Cu under alkaline conditions at room temperature, and hydrogen can be obtained. However, because of their high surface energies of Cu nanoparticles, the activity components of the catalysts tend to congregate

---

[*] Corresponding author. Tel.: +86 10 64419619; fax: +86 10 64419619.
E-mail address: jisf@mail.buct.edu.cn (S. Ji).

0920-5861/$ – see front matter © 2010 Elsevier B.V. All rights reserved.
doi:10.1016/j.cattod.2010.03.074

and/or change in catalytic reactions. They eventually lose the initial activity and selectivity. If the Cu nanoparticles assemble on the surface of $Fe_3O_4@SiO_2$, the conglomeration of the Cu nanoparticles can easy be solved. At the same time, the catalysts can also be effectively separated and reused under magnetic field.

In this study, the core–shell structured $Cu/Fe_3O_4@SiO_2$ microsphere catalysts, in which the Cu nano-grain active component was embedded on the mesoporous SiO_2 shell layer, were prepared. The structure of the samples was characterized by X-ray diffraction, transmission electron microscopy, N_2 adsorption–desorption isotherms and vibration sample magnetometer technique. The catalytic activity of the hydrogen produced from low concentration formaldehyde solution was evaluated. This strategy retained the Cu nanoparticles of the catalysts and the formaldehyde can produce hydrogen under mild reaction conditions.

2. Experimental

2.1. Preparation of sample

2.1.1. Preparation of Fe_3O_4

Typically, using CTAB as surfactant, 60 mL of $FeCl_2$ and $FeCl_3$ aqueous ethanol solution with a concentration ratio of 5:1 was prepared, 1.0 mol/L ammonia solution was added drop by drop with vigorous stirring until pH 10, and a black product was obtained. Then, the black product was crystallized under 50 °C water bath for 3 h. Subsequently, separated with magnet, the obtained black magnetite particles were washed with ethanol for 3 times, dried at 50 °C for 12 h.

2.1.2. Preparation of $Fe_3O_4@SiO_2$

The core–shell $Fe_3O_4@SiO_2$ microspheres were prepared by a modified sol–gel method. Briefly, 0.50 g Fe_3O_4 was dispersed into 50 mL 0.1 M HCl aqueous solution, ultrasonic for 10 min, separated with a magnet and washed with deionized water for 3 times, and then homogeneously dispersed in a mixture of 80 mL ethanol, 20 mL deioned water and 2.0 mL 28 wt% ammonia aqueous solution, followed by the addition of TEOS 0.20 mL. Stirring at room temperature for 6 h, the product separated with a magnet and washed with deionized water for 3 times, dispersed in a mixed solution containing 80 mL ethanol, 60 mL deionized water, 2.0 mL 28 wt% ammonia aqueous solutions and 0.500 g CTAB, stirred for 1 h, and then 1.00 mL tetraethyl orthosilicate was added. After stirring for 6 h, the product was separated with magnet and washed by deionized water and ethanol, dried at 50 °C for 12 h.

2.1.3. Preparation of $Cu/Fe_3O_4@SiO_2$

Firstly, a certain concentration of copper acetate aqueous solution was prepared. 0.50 g $Fe_3O_4@SiO_2$ was dispersed in the blue solution, ultrasonically for 15 min. 28 wt% ammonia aqueous solution was added dropwise until pH 13, and then hydrazine hydrate was added until a brown aqueous solution appeared. Stewing for 10 min, the product was separated with magnet and washed by ethanol for 3 times, dried at 50 °C for 12 h. A series of $Cu/Fe_3O_4@SiO_2$ catalysts with different Cu contents (5 wt%, 10 wt% and 15 wt%) were prepared.

2.2. Characterization of samples

The X-ray diffraction (XRD) patterns were recorded using a D/Max 2500 VB2+/PC diffractometer with Cu Ka irradiation ($\lambda = 1.5418$ Å) at 200 kV and 50 mA in the range of 2θ value between 10° and 90° with a speed of $10^\circ\ min^{-1}$. Transmission electron microscopy (TEM) observation was performed on an JEM 3010 transmission emission microscope operated at a 300 kV accelerating voltage. Magnetic properties of the samples were measured using a vibration sample magnetometer (VSM; Lake Shore Model 7400) under magnetic fields up to 20 kOe. The N_2 adsorption–desorption isotherms was tested on ASAP2020 M automatic specific surface area and aperture analyzer. The samples were pretreated at 300 °C for 4 h and the specific surface area of samples determined using the Brunauer–Emmett–Teller (BET) method. The pore volume and pore size distribution were derived from the desorption profiles of the isotherms using the Barrett–Joyner–Halanda (BJH) method.

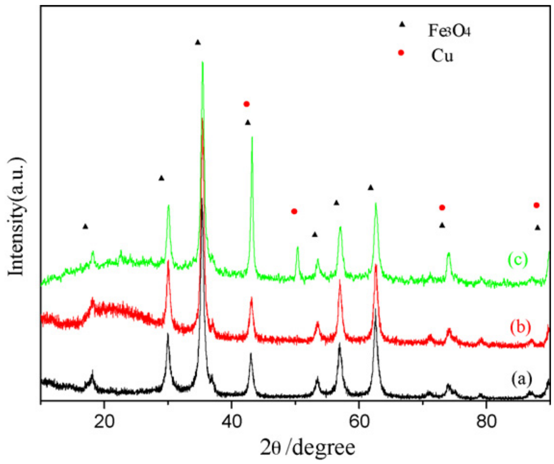

Fig. 1. The large-angle XRD patterns (a) Fe_3O_4 particles, (b) $Fe_3O_4@SiO_2$ microspheres, (c) 15%$Cu/Fe_3O_4@SiO_2$ catalyst.

2.3. Catalytic activity measurement

The catalytic reaction was carried on a self-made continuous stirred liquid–solid catalytic reactor. The temperature of the reaction was controlled by circulating water, about 25 °C. The volume of generation gas was measured by drainage. 100 mL 15 g/L formaldehyde solution was added into the reactor, was stirred, and 0.1 g $Cu/Fe_3O_4@SiO_2$ catalyst and 4.0 g NaOH were added. The hydrogen generated after dry was analyzed on-line with gas chromatography. The catalytic properties of $Cu/Fe_3O_4@SiO_2$ catalyst were measured by the volume of hydrogen generation. The recyclability of catalyst was investigated and the catalyst without further treatment.

3. Results and discussion

3.1. XRD

The large-angle XRD patterns of (a) Fe_3O_4 and (b) $Fe_3O_4@SiO_2$ as well as (c) $Cu/Fe_3O_4@SiO_2$ are shown in Fig. 1. It can be seen that the Fe_3O_4 obtained have highly crystalline cubic spinel structure agreed well with the standard Fe_3O_4 (cubic phase) XRD spectrum (PDF#88-0866). From Fig. 1(b), we can see that the XRD pattern of $Fe_3O_4@SiO_2$ prepared by Stöber process is similar to the pattern of Fe_3O_4 [1] and shows a obviously diffusion peak at $2\theta = 15–25^\circ$, generally considered as the diffusion peak of amorphous silica. Fig. 1(c) represents the XRD pattern of $Cu/Fe_3O_4@SiO_2$ catalyst, showing that the peaks of both Fe_3O_4 and Cu appear and some enhanced peak intensity is caused by overlapping of peaks. The Cu peaks of $Cu/Fe_3O_4@SiO_2$ catalyst agree well with the standard Cu (cubic phase) XRD spectrum (PDF#04-0836).

The low-angle XRD patterns of samples are respectively shown in Fig. 2a–c. The (1 0 0) diffusion peak appeared at $2\theta = 2.4^\circ$, suggesting that $Fe_3O_4@SiO_2$ and $Cu/Fe_3O_4@SiO_2$ had mesoporous structure, which may be formed in the amorphous silica shell.

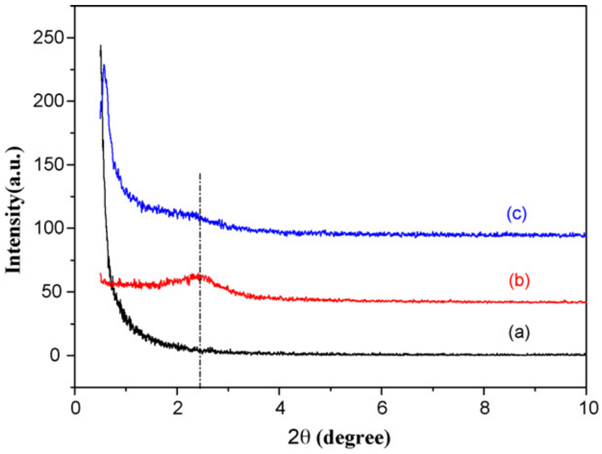

Fig. 2. The low-angle XRD patterns of (a) Fe_3O_4 particles, (b) Fe_3O_4@SiO_2 magnetic microspheres, (c)15% Cu/Fe_3O_4@SiO_2 catalyst.

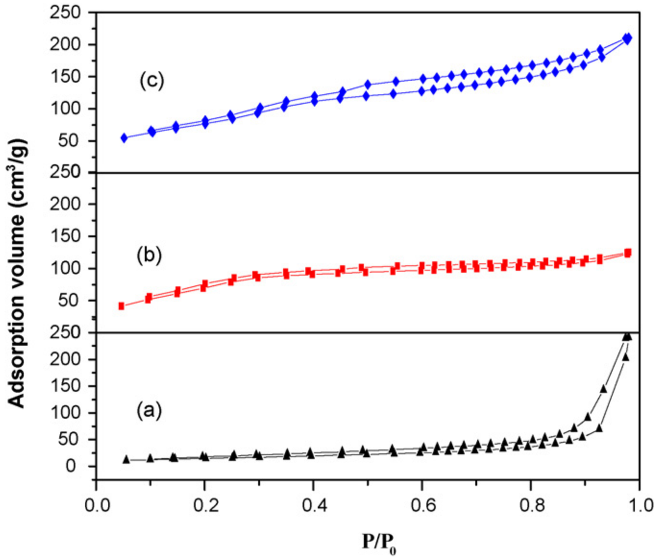

Fig. 3. N_2 adsorption–desorption isotherms of (a) Fe_3O_4 particles, (b) Fe_3O_4@SiO_2 magnetic microspheres, (c) 15%Cu/Fe_3O_4@SiO_2 catalyst.

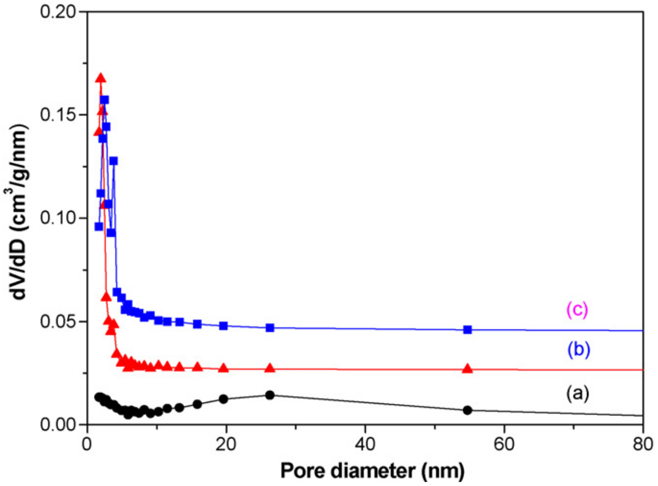

Fig. 4. Pore size distributions of (a) Fe_3O_4, (b) Fe_3O_4@SiO_2, (c)15% Cu/Fe_3O_4@SiO_2.

3.2. BET

The N_2 adsorption–desorption isotherms of (a) Fe_3O_4 and (b) Fe_3O_4@SiO_2 as well as (c) Cu/Fe_3O_4@SiO_2 are shown in Fig. 3. A linear increase was found in the amount of adsorbed nitrogen at a low relative pressure. According to the IUPAC, it can be classified as a type of H2 hysteresis loops, and both Fe_3O_4@SiO_2 and Cu/Fe_3O_4@SiO_2 catalyst exhibited IV-type curves (Fig. 3b and c). The mesoporous size distribution exhibited a sharp peak centered at the mean value of 1.9 nm for microspheres and the Cu catalyst system showed two peaks at 2.4 nm and 3.8 nm when calculated by Barrett–Joyner–Halenda (BJH) method (Fig. 4). The peak at 3.8 nm may be caused by the accumulation of Cu/Fe_3O_4@SiO_2 catalyst. Table 1 is the textural and structural characteristics of the samples, from Table 1 we can see the BET surface area of Fe_3O_4@SiO_2 and Cu/Fe_3O_4@SiO_2 catalyst is respectively 281.4 m^2/g and 287.7 m^2/g as calculated by the Brunauer–Emmett–Teller (BET) method. The BJH desorption cumulative volume is respectively 0.29 cm^3/g and 0.33 cm^3/g as calculated by the Barrett–Joyner–Halanda (BJH) method.

Table 1
Textural and structural characteristics of the samples.

Samples	Sg_{BET} (m^2/g)	Vg_{BJH} (cm^3/g)	Dv (nm)
Fe_3O_4	54.7	0.38	27.0
Fe_3O_4@SiO_2 microspheres	281.4	0.29	1.9
15% Cu/Fe_3O_4@SiO_2 catalyst	287.7	0.33	2.4, 3.8

3.3. TEM

Fig. 5 shows the TEM images of (a) Fe_3O_4 and (b) Fe_3O_4@SiO_2 as well as (c) Cu/Fe_3O_4@SiO_2 catalyst. It was found that the Fe_3O_4 nanoparticles obtained diameter about 15 nm with narrow size range, corresponding with the result calculated by Scherrer equation. The Fe_3O_4@SiO_2 microspheres were obtained with a diameter of about 500 nm because of agglomeration of Fe_3O_4 inside microspheres and surface growth of silica on the shell [16]. The internal structure cannot be clearly seen due to the larger particle size of microspheres, which cannot be broken down by electron beam from transmission electron microscopy. The nano-Cu combined with the surface of magnetic microspheres on form of embedding and theirs diameter about 10 nm, ensured the Cu nano-grains uneasy to loss when reused in liquid phase catalytic reaction.

3.4. VSM

Fig. 6 shows the magnetic hysteresis loops of samples. It indicated that all products had superparamagnetism. The magnetization curve and demagnetization curve are coincident, no hysteresis phenomenon was found, and remanent magnetization and coercivity are equal to zero. The Fe_3O_4 was obtained with maximum saturation magnetization 83.2 emu/g (Fig. 6a), the hysteresis loops of Fe_3O_4@SiO_2 and Cu/Fe_3O_4@SiO_2 are substantially accordant, for a spot of nano-Cu cannot distinctly affect the magnetic properties of Cu/Fe_3O_4@SiO_2 catalyst. Their maximum saturation magnetization is respectively 24.0 emu/g and 20.7 emu/g (Fig. 6b and c).

3.5. Catalytic activity

3.5.1. The effect of Cu content on the catalytic performance of catalyst

Fig. 7 shows the relationship curves between the Cu content of catalyst and the hydrogen generation volume. From the figure we can see, the rate of hydrogen generation was greatly dependent on the content of Cu, the rate of hydrogen generation increased when Cu content increased from 5 wt% to 20 wt%; however, when the

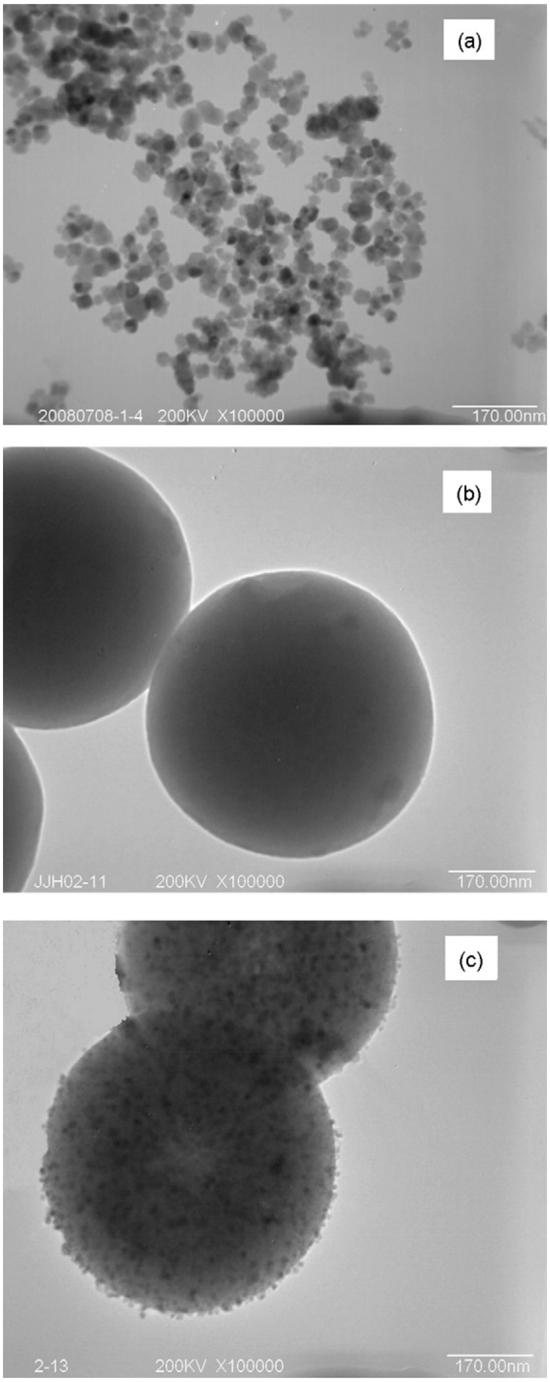

Fig. 5. TEM images of (a) Fe_3O_4 particles, (b) Fe_3O_4@SiO_2 magnetic microspheres, (c) 15% Cu/Fe_3O_4@SiO_2 catalyst.

content of Cu was more than 15%, the rate of hydrogen generation volume scarcely increased, maybe it is because of the dispersion morphology of Cu nano-grains on the surface of microspheres, while the content of Cu is low, the surface of microspheres cannot be studded, when the content of Cu increases to a certain degree, the Cu nano-grains would be densely covered on the surface of microspheres, further increasing the content of Cu that cannot acquire more better catalytic activity.

3.5.2. The effect of catalyst dosage on the catalytic performance of catalyst

Fig. 8 shows the relationship curves between the hydrogen generation volume and the amount of catalyst and the volume of hydrogen generation increased with the increase of catalyst dosage, when the catalyst dosage was respectively 0.10 g and 0.20 g, both got the maximum of hydrogen generation 42 mL when the reaction proceeded for 45 min, but the initial rate of hydrogen generation decreased with the decrease of catalyst dosage, while the input amount of catalyst was 0.05 g, the rate of hydrogen generation decreased significantly, and took more than 1 h to get the maximum volume of hydrogen 38 mL. With the increase of reaction time, the concentration of formaldehyde decreased gradually, all results indicated that the catalytic hydrogen reactions involve the surface reaction of HCHO adsorbed on the (1 1 1) crystal planes of Cu nano-grain [17], the dosage of catalysts can affect the rate of hydrogen generation.

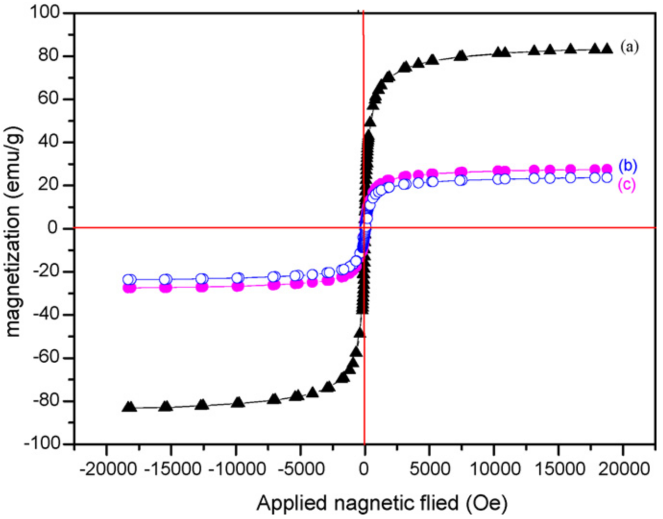

Fig. 6. VSM hysteresis loops of (a) Fe_3O_4 particles, (b) Fe_3O_4@SiO_2 magnetic microspheres, (c)15% Cu/Fe_3O_4@SiO_2 catalyst.

3.5.3. The effect of NaOH concentration on the catalytic performance of catalyst

Fig. 9 shows the relationship curves between the NaOH concentration and the hydrogen generation volume. From the figure we can see, with the increase of NaOH concentration, the rate of hydrogen generation increased and when the NaOH concentration was 2.0 mol/L, the initial rate of hydrogen generation decreased, and the reaction proceeded for 1 h, the volume of hydrogen generation was

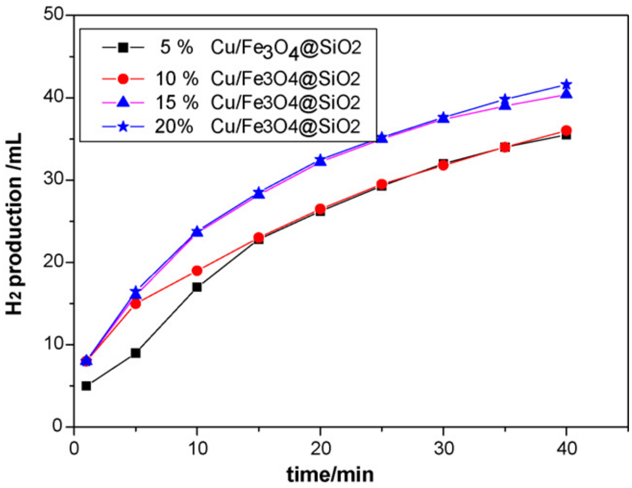

Fig. 7. The relationship curves between the Cu content of catalyst and the hydrogen generation volume.

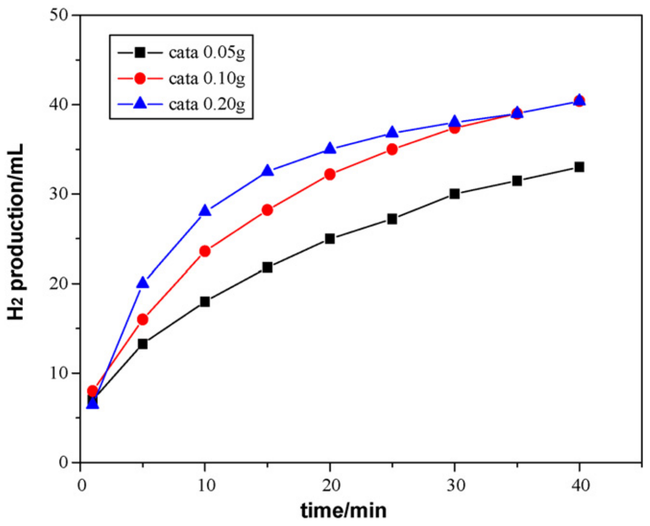

Fig. 8. The relationship curves between the hydrogen generation volume and the amount of catalyst.

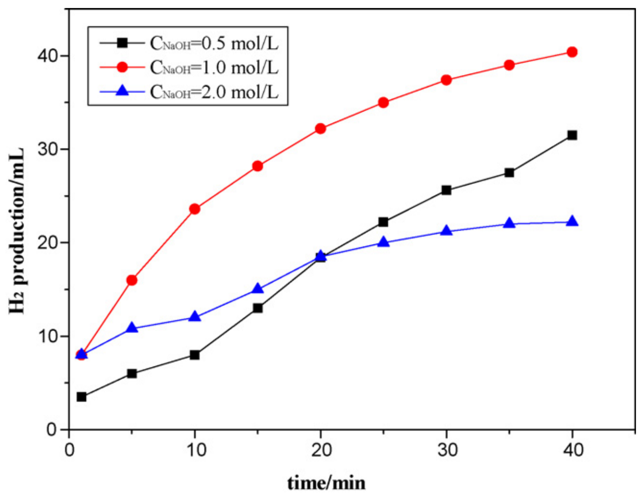

Fig. 9. The relation curves between the NaOH concentration and the hydrogen generation volume.

just about 22 mL, which might be due to the competition reaction of formaldehyde via Cannizzaro reaction [18].

3.5.4. *The effect of reuse time of catalyst on the catalytic performance of catalyst*

The relationship curves between the reuse time of catalyst and the hydrogen generation volume are shown in Fig. 10. With the reuse time increasing, the maximum volume of hydrogen generation has no obvious decrease. Even after using for 8 times, the maximum volume of hydrogen generation was still maintained at 34 mL. The hydrogen generation volume decreased by 15% and the loss quantity of catalyst was about 2.0%, it indicated that the Cu/Fe_3O_4@SiO_2 catalyst has higher stability.

4. Conclusion

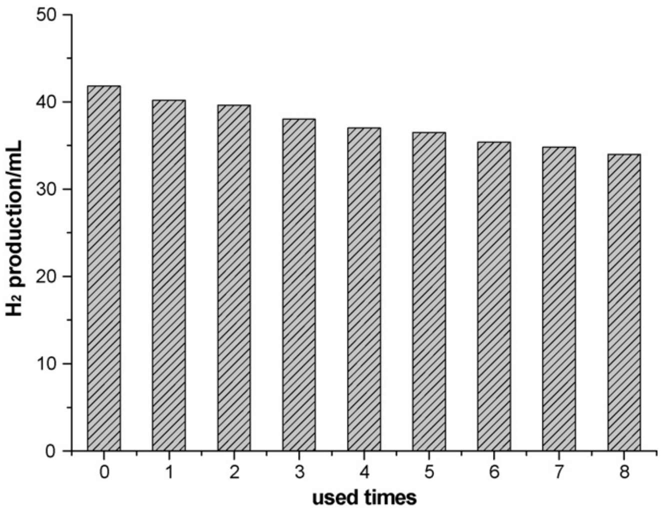

Fig. 10. The relationship curves between the reuse time of catalyst and the hydrogen generation volume.

Fe_3O_4 was successfully prepared by coprecipitation with $FeCl_2$ and $FeCl_3$ as reaction substrate, CTAB as surfactant, ethanol solution as solvent, and aqueous ammonia as precipitant. The Fe_3O_4@SiO_2 was obtained according to the typical Stöber process. Cu/Fe_3O_4@SiO_2 catalyst was obtained by reducing copper ammonia complexes using hydrazine hydrate on the surface of Fe_3O_4@SiO_2 microspheres. The characterization results showed that the diameter of Fe_3O_4 obtained is about 15 nm, and the size of Fe_3O_4@SiO_2 and Cu/Fe_3O_4@SiO_2 microspheres was about 500 nm, the diameter of Cu nanoparticles on the surface of Fe_3O_4@SiO_2 microspheres was 10 nm. All samples presented a high degree of superparamagnetism, the maximum saturation magnetization of Cu/Fe_3O_4@SiO_2 catalysts was still kept at 20.7 emu/g. Both the Fe_3O_4@SiO_2 microspheres and the Cu/Fe_3O_4@SiO_2 catalysts had mesoporous structure. The catalytic performance for catalyzed formaldehyde hydrogen generation was researched at room temperature. When the content of Cu was about 15%, the catalyst exhibited the best catalytic activity; the accumulative generation amount of H_2 reached 42 mL in 45 min. After running recycling for 8 times, the catalyst still exhibited high catalytic activity.

Acknowledgement

Financial funds from the National Natural Science Foundation of China (project 20473009) are gratefully acknowledged.

References

[1] Y.H. Deng, D.W. Qi, C.H. Deng, X.M. Zhang, D.Y. Zhao, J. Am. Chem. Soc. 130 (2008) 28.
[2] X.Q. Xu, C.H. Deng, M.X. Gao, W.J. Yu, P.Y. Yang, X.M. Zhang, Adv. Mater. 18 (2006) 3289.
[3] D.D. Shao, K.K. Xu, X.J. Song, J.H. Hu, W.L. Yang, C.C. Wang, J. Colloid Interface Sci. 336 (2009) 526.
[4] M.J. Jacinto, O.H.C.F. Santos, R. Landers, P.K. Kiyohara, L.M. Rossi, Appl. Catal. B 90 (2009) 688.
[5] M.J. Jacinto, O.H.C.F. Santos, R.F. Jardim, R. Landers, L.M. Rossi, Appl. Catal. A 360 (2009) 177.
[6] J.P. Ge, Q. Zhang, T.R. Zhang, Y.D. Yin, Angew. Chem. Int. Ed. 47 (2008) 8924.
[7] X.J. Tang, Y. Bai, A. Duong, M.T. Smith, L.Y. Li, L.P. Zhang, Environ. Int. 35 (2009) 1210.
[8] G.J. Millar, C.H. Rochester, K.C. Waugh, J. Catal. 155 (1995) 52.
[9] W.H. Hung, S.L. Bernasek, Surf. Sci. 346 (1996) 165.
[10] R. Stadler, Z. Jusys, H. Baltruschat, Electrochim. Acta 54 (2009) 5408.
[11] D.H. Mei, N.A. Deskins, M. Dupuis, Surf. Sci. 601 (2007) 4993.
[12] B.T. Teng, S.Y. Jiang, Z.X. Yang, M.F. Luo, Y.Z. Lan, Surf. Sci. 604 (2010) 68.
[13] L. Kieu, P. Boyd, H. Idriss, J. Mol. Catal. A: Chem. 176 (2001) 117.
[14] S.G. Sun, G.Q. Lu, Z.W. Tian, J. Electroanal. Chem. 393 (1995) 97.
[15] Y.P. Bi, G.X. Lu, Int. J. Hydrogen Energy 33 (2008) 2225.
[16] J. Kim, J.E. Lee, J. Lee, J.H. Yu, B.C. Kim, K. An, Y. Hwang, C.H. Shin, J.G. Park, J. Kim, T. Hyeon, J. Am. Chem. Soc. 128 (2006) 688.
[17] J.R.B. Gomes, J.A.N.F. Gomes, F. Illas, J. Mol. Catal. A: Chem. 170 (2001) 187.
[18] H. Nakayama, A. Hayashi, T. Eguchi, N. Nakamura, M. Tsuhako, Solid State Sci. 4 (2002) 1067.